

Article

The Implication of Petrographic Characteristics on the Mechanical Behavior of Middle Eocene Limestone, 15th May City, Egypt

Abdelaziz El Shinawi ¹, Peter Mésáros ² and Martina Zelenáková ^{3,*}

¹ The Environmental Geophysics Lab (ZEGL), Department of Geology, Faculty of Science, Zagazig University, Zagazig 44511, Egypt; geoabdelaziz@yahoo.com

² Institute of Technology, Economics and Management in Construction, Faculty of Civil Engineering, Technical, University of Košice, 042 00 Košice, Slovakia; peter.mesaros@tuke.sk

³ Institute of Environmental Engineering, Faculty of Civil Engineering, Technical, University of Košice, 042 00 Košice, Slovakia

* Correspondence: martina.zelenakova@tuke.sk

Received: 19 October 2020; Accepted: 13 November 2020; Published: 20 November 2020



Abstract: The construction purposes of carbonate rocks are considered a major aspect of using these bedrocks based on their mechanical behavior. Accordingly, the physical and mechanical characterization of Middle Eocene Limestone bedrock in the new urban area at the 15th May City, Egypt was studied to assess the suitability of the carbonate rocks for construction. This study has been carried out to investigate the effect of petrographic characteristics on mechanical properties. To achieve this objective, the intact 30 rock core samples from 15 boreholes were selected at different depths. Based on study of the selected samples in thin sections, the limestone in the area was classified as lime-mudstone, wackestone, and grainstone. Additionally, the uniaxial compressive strength (UCS) and Schmidt Rebound Hammer (Rn) were determined to detect the mechanical properties of the limestone bedrock. The measured parameters (UCS and Rn) demonstrated a high direct relationship with mudstone and a poor direct relationship with dolomite and high negative correlation with wackestone and grainstone. Therefore, the Middle Eocene Limestone bedrock is more durable and has medium-strength, which made it suitable for constructions. Regression analysis was performed to find out some linear relationship between mechanical properties (UCS) with petrographic characteristics. The study reveals significant positive correlation between UCS and Rn with mudstone in accordance higher values of regression coefficient ($R^2 = 0.91$ and $R^2 = 0.036$), and an inverse relationship of Rn with dolomite % ($R^2 = 0.89$ and $R^2 = 0.02$), respectively. Consequently, the strong confidence on the mechanical parameters opens the way for engineers to predict the mechanical parameters that are required for engineering properties of limestone for the urban expansion.

Keywords: lime-mudstone; unconfined compressive strength; Schmidt hammer; wackestone

1. Introduction

Generally, limestone has been considered the main bedrock for roads, bridges, and tunnels construction, slope protection engineering, and water conservancy [1–3]. Recent expansion of the urban area over the surrounding desert land has directed the attention to investigate both the engineering and geological constrains on these new developments. This city was constructed on Eocene limestone beds intercalated with thin beds of clay and very thin beds of salt. In general, the Eocene limestone sediments in Egypt are characterized by karstification phenomena causing fractures, cracks, cavities, and land subsidence.

Peak strength and mechanical deformation characteristics of limestone directly relate to these projects' stability and is therefore helpful to forecast risk [4–7]. Furthermore, research on the behavior of limestone under natural and experimental conditions is helpful in explaining rheological characteristics of upper crustal rocks, chemical and physical effects of fluid in geologic processes, the meaning of tectonophysics, structural adjustment of the upper crust, and dynamic processes of fault zone formation and evolution with fluid; it is also helpful in explaining seismogenic mechanisms and seismic wave propagation [8–11]. The study area, located at the northern part of 15th May City, 12 km to the southeast of Cairo, is one of the promised cities planned in 1986 by the Egyptian government through its program to withdraw the population from the condensed. It was proposed for the installation of a new industrial zone that shall contain housing and manufacturing facilities. New urban communities are located in the study area, some of which are in close proximity to such quarry locations such as 15th May city, south of Helwan City. Being constructed over a limestone plateau, the city is surrounded by an old quarry, which was moved to a distance of 5 km away from the city (Figure 1). Such quarry has been operated on a faulted area with weak zones of brittle materials [12]. The area encompasses seven new cities that have been partially constructed during the last decades. The cities are 10th Ramadan, El Ebour, New Cairo, El Amal, El Sherouk, 15 May, and Badr. Seven factors triggering landslides—slope angles, rock type, faults, elevation, seismic intensity zones, stream density, and land cover—were input to the model to produce a landslide susceptibility map. Such a map was used to examine the susceptibility of the locations of the seven new cities. The result revealed the high vulnerability of the locations of El Amal and 15 May Cities and a few zones including south of Cairo city [13,14]. In geotechnical and engineering projects, rock classifications are based on mechanical parameters such as uniaxial compressive strength (UCS), Point load, and Schmidt Rebound Hammer (Rn). These parameters are most widely used and adequate to characterize the mechanical behavior of rocks. The development of construction occupation increases the demands of construction materials and necessitates study on all sides of petrographic and mechanical properties of various rocks. Mechanical properties of intact rocks are greatly influenced by their textural characteristics. However, many researchers have conducted mineralogical studies on the limestone rocks [15–19]. Aggregate degradation (AD) commonly decreases particle angularity, surface texture, and size, and also diminishes the shear strength and grade of aggregate materials. In this case, AD is one of the main reasons accounting for the failure mechanism of aggregate materials. It is possible to predict AD properties from each kind of rock strength test based on rock types. Accordingly, using the equations obtained by tests to estimate the AD can be more economical and practical, especially in prefeasibility study, to predict the limits of allowable AD values for practical applications [20,21]. On the other hand, the validity of rocks to be used as construction material is the function of its mineralogical composition [16,22]. UCS of rocks aggregate is indirectly related to their mineral constituents, bioclasts, cement, and texture. Physical properties and mechanical behavior of rocks are influenced by modal mineral composition and grain size [23]. Physical properties of construction materials are directly related to UCS, mineralogical, and textural characteristics of rocks. Consequently, tests of the physical and mechanical properties were conducted for the collected rock core samples for determining the relation between mechanical behavior and mineralogical composition [6]. This study has been carried out to investigate the effect of petrographic characteristics on mechanical properties. These relations have their own effect for predicting the rock strength characteristic and their suitability for different engineering structures in 15th May City, southeast Cairo, for construction purposes, which are in close proximity to such quarry locations (Figure 1).

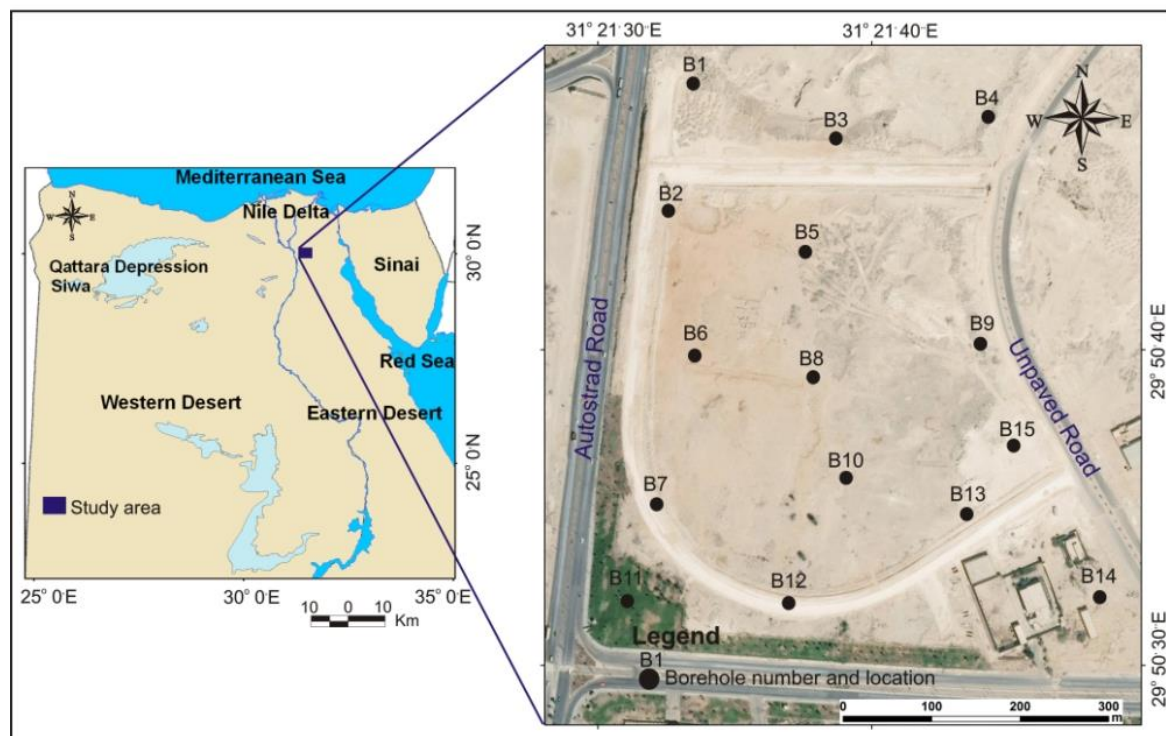


Figure 1. Location map of the study area and the drilled boreholes.

2. Geologic Setting

Topographically, the area has two plateaus separated by a topographically low area. Gabal Mokattam forms the northern plateau and is separated from the southern plateau by a topographically low area that is occupied by El-Maadi-Qatamia road [24].

The northern plateau slopes gently northwards where it disappears under the Oligocene sands and gravels of Gebel El-Ahmer. A relatively high escarpment and its northern side mark the southern plateau. It is known here as Tura-Hof-Observatory plateau. The Middle Eocene beds are mainly composed of limestone. These beds are found to be either unfossiliferous or containing badly preserved fossils. These beds were divided into two formations from bottom to top: The Gebel Hof and Observatory Formations. A brief description of both formations is as follows.

The stratigraphic succession of the study area is subdivided into the Mokattam and Maadi Groups. The Mokattam group is composed of the Gebel Hof Formation; it is the oldest exposed rock unit in the study area. It accomplishes about 121 m thick and is composed of white limestone, fine to medium, hard, and medium to thick bedded lithological unit (Figure 2). Observatory Formation: Stratigraphically, it is the highest formation of the Middle Eocene age. It is mainly composed of chalky and marly limestone forming the main quarrying horizons at Helwan town and the neighborhood. This formation is typically developed below the Helwan Observatory, forming the entire Observatory plateau and extending to the north where it is thrown down against the Gebel Hof Formation. It is made up of 136 m limestone and chalky limestone of different lithologies and textures. It is burrowed, laminated, thin bedded, and weathered. Consequently, in the Maadi group, these Upper Eocene sediments are overlying the Middle Eocene Mokattam group in the study area. It is divided into three formations; Qurn Formation is composed of 97 m thick sequence of marly and chalky limestone alternating with shales, sandy marls. Wadi Garawi Formation is composed of a 25 m thick poorly fossiliferous sandy shale section with a hard highly fossiliferous middle bed. Wadi Hof Formation is made up of the Late Eocene sediments that are composed of limestone, clays, marl, and sandstone, 65 m thick.

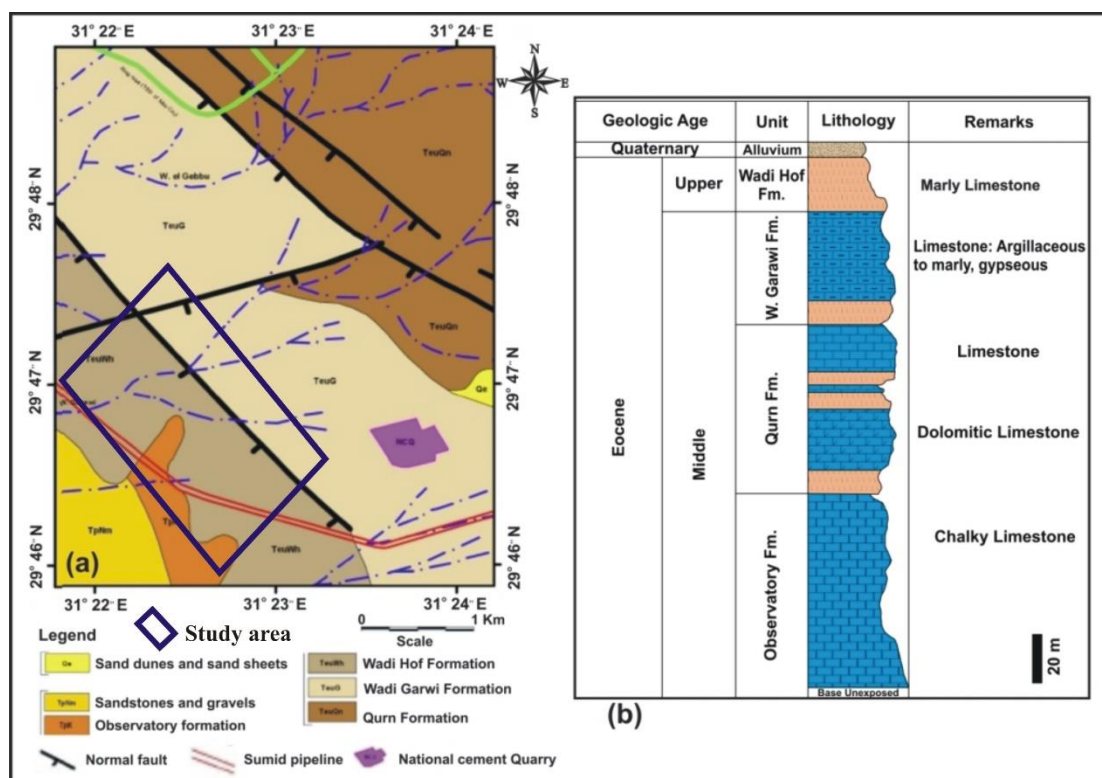


Figure 2. (a) Geologic map of the northern part of 15th May City and (b) stratigraphic column showing the geological setting [13].

3. Materials and Methods

The mechanical behavior of the limestone samples was performed by the field and laboratory work. The field work represents rock sampling along the study area (Figure 1).

A total of 30 continuous core samples, intended to be representative of the foundation bedrock, 50 to 70 mm in diameter, were extracted from 15 boreholes with depths that ranged between 10 and 30 meters using diamond core bit fixed on rotary drilling machine. An extensive laboratory testing program was encountered to define the physical, mechanical properties, and petrographic characteristics of the rock material for the foundation bedrock. Consequently, the physical properties of the limestone samples along the study site were performed; water content [25], density [26], and specific gravity [27]. Furthermore, the mechanical parameters of the limestone intact core samples were determined by using the Schmidt rebound hammer and uniaxial compressive strength. The Schmidt hammer test was performed within 5° of vertical with the bottom of the piston at right angles to, and in firm contact with, the surface of the test specimen [28]. The Schmidt rebound hammer test was performed on N-type rock core specimens. Rock core specimens were steadily fixed in a steel cradle with a semi cylindrical machined slot of the same radius as the core, or firmly seated into a steel V-shaped block. Core rock samples, with a length-to-diameter ratio of 2.5–3.0, were prepared and flattened up to 0.02 mm with both sides smooth for uniaxial compression testing following the specifications of previous authors [29,30]. Since all the UCS tests were conducted on an NX sized core (54 ± 1 mm), all results were corrected by using relation [31] to rule out the influence of specimen volume. Selected representative intact core specimens of Middle Eocene limestones were prepared and tested for measuring their mechanical properties under uniaxial compression. A universal testing machine (Instron, Model 1128) was used for these tests. The loading system of this machine is a controlled strain type giving deformation speeds from 0.05 mm/min to 500 mm/min. The compressive force produced by this machine ranges from 10 gm to 50 Kg. The testing machine is provided with a plotter for producing testing. Additionally, the petrographical study of the selected samples was performed whereby five thin sections were

prepared, examined under a microscope, and the limestone samples were classified. The limestones were examined by a Laboval-3 optical microscope in transmitted plane- (PPL) and cross-polarized light (XPL) to perform a semi-quantitative analysis of the components (texture, matrix composition, and grain types). Micrographs were simultaneously acquired by a Nikon Coolpix 990 digital camera at 1.2 megapixel. Limestone samples were categorized according to the classification of depositional textures of carbonate rocks proposed [29].

4. Results

4.1. Study Site Description

Three main rock types of layers were observed from the boreholes and the cross sections (Figure 3) as follows.

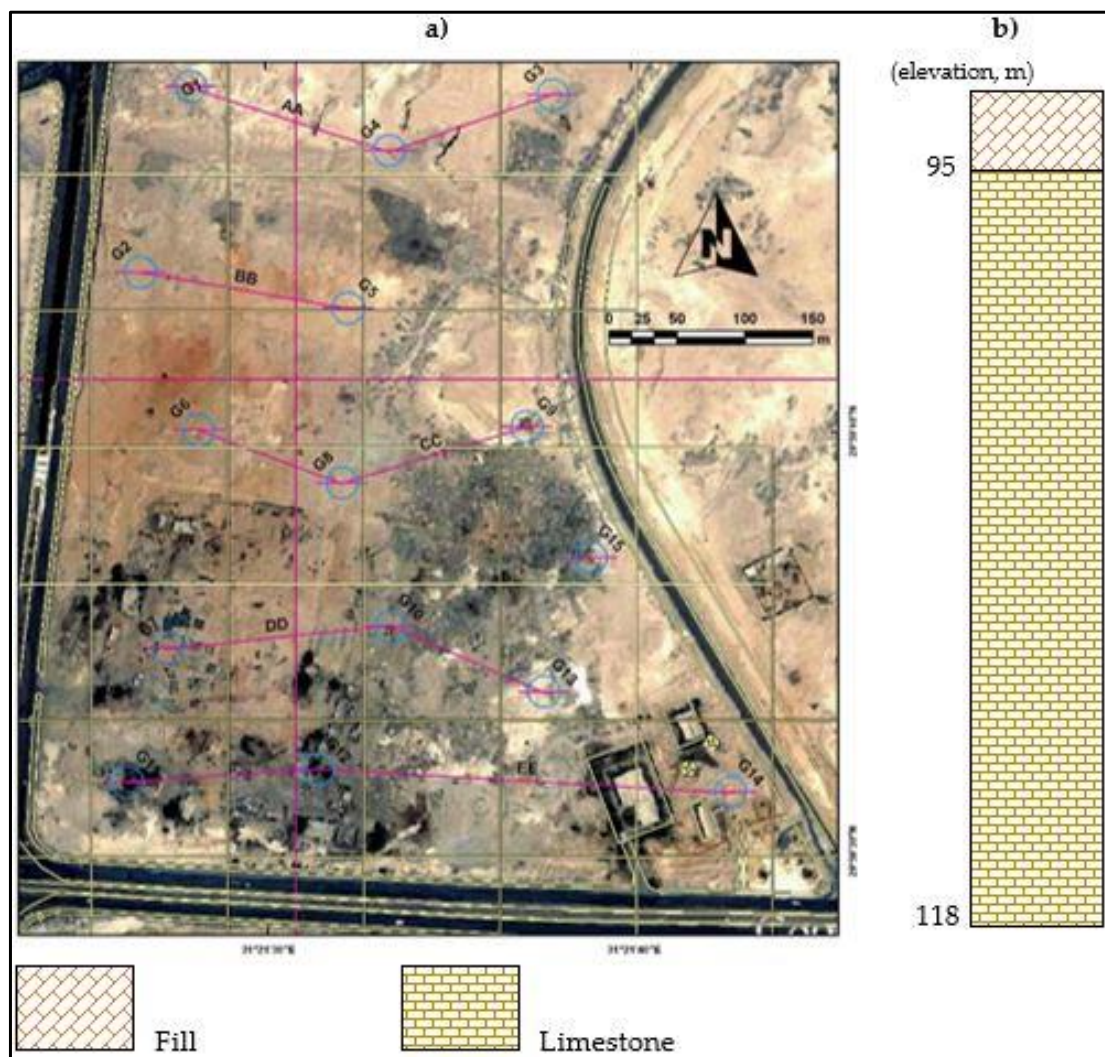


Figure 3. (a) Drilled boreholes locations and cross sections; (b) composite log from the drilled boreholes in the study site based on collected intact rock samples.

Surface layer characterizes overburden materials and composed of weathered limestone. The average thickness of this layer varies between 0.7 and 3 m. The middle layer is composed of argillaceous limestone facies with thickness ranges between 0.5 to 30 m. The bottom layer is characterized by highly argillaceous limestone bedrock with pockets of marl intercalations

4.2. Petrographic Characteristics and Depositional Environment

The investigated Middle Eocene limestone rock samples were texturally classified according to [29] into lime-mudstone, wackestone, and grainstone (Table 1). The major component, lime-mudstone, shows a high percentage of mud and fine materials, which varied in the range of 43% to 85% with a mean of 63.8% and a standard deviation of 13.64. However, wackestone was represented with a high percentage of grains in the range of 4% to 28% with a mean of 15.1% and a standard deviation of 7.09. The lime-mudstones are argillaceous and made up of shells from 1% to 7%. The matrix contains micrite with fine-grained materials, and secondary fissures are visible as white spots (Figure 4a). On the other hand, the wackestone carbonate rocks contained more than 10% calcite grains informed in micritic matrix and the matrix was recrystallized into sparry calcite (Figure 4b). The percent of grainstone ranged from 8% to 30% with and the Mean is 18.8%. The grainstone are argillaceous and made up of shells (10–40%) set in a micritic matrix. (Figure 4c). Dolomite was presented with a very low percent in fine material matrix, which varied in the range of 0% to 3% with a mean of 2.01 and a standard deviation of 2.01 (Figure 4d).

Table 1. Middle Eocene Limestone composition, uniaxial compressive strength (UCS) and Schmidt Rebound Hammer (Rn) values.

Sample No.	Depth	Location	Limestone Composition				Classification Name	UCS (MPa)	Rn
			Grains <10%	Grains >10%	Dol (%)	Lacks Mud (%)			
S1	20	BH4	7	78	7	8	Mudstone	40.29	31
S2	15	BH2	10	70	0	19	Wackestone	38.55	30
S3	7	BH5	13	65	2	20	Wackestone	37.11	28
S4	12	BH10	16	50	5	28	Wackestone	35.22	26
S5	20	BH15	20	55	2	23	Wackestone	35.00	26
S6	5	BH3	12	60	0	18	Wackestone	36.44	27
S7	2	BH6	10	69	0	19	Wackestone	38.15	30
S8	23	BH7	20	57	2	21	Wackestone	34.26	25
S9	15	BH9	25	45	2	28	grainstone	32.69	25
S10	22	BH5	4	82	1	13	Wackestone	36.25	31
S11	2	BH8	16	50	5	28	Wackestone	35.22	26
S12	16	BH3	10	75	4	9	Mudstone	39.16	32
S13	18	BH14	5	85	0	9	Mudstone	35.66	32
S14	5	BH2	15	68	3	14	Wackestone	37.2	28
S15	4	BH5	26	51	0	23	grainstone	34.66	25
S16	14	BH11	28	47	2	23	grainstone	31.66	26
S17	16	BH3	6	79	0	15	Wackestone	41.55	33
S18	22	BH7	17	68	3	14	Wackestone	36.52	27
S19	27	BH10	23	47	0	30	grainstone	31.50	25
S20	6	BH9	15	65	3	17	Wackestone	36.27	27
S21	9	BH15	5	85	0	9	Mudstone	34.26	32
S22	3	BH13	17	70	6	9	Mudstone	38.82	32
S23	7	BH9	26	49	0	25	Wackestone	34.66	25
S24	12	BH1	7	75	2	16	Wackestone	40.22	31
S25	2	BH1	5	84	1	10	Mudstone-wackestone	43.22	31
S26	28	BH15	25	45	3	27	Wackestone	33.52	24
S27	4	BH14	26	51	0	23	Wackestone	34.66	25
S28	6	BH1	8	76	1	15	Wackestone	38.55	30
S29	1	BH7	27	43	0	30	grainstone	29.16	23
S30	12	BH1	9	70	0	21	Wackestone	38.27	29
Mean	-	-	15.10	63.80	1.8	18.08	-	36.29	28.07
Stdev			7.09	13.64	2.01				

(UCS) uniaxial compressive strength and (Rn) Schmidt rebound hammer.

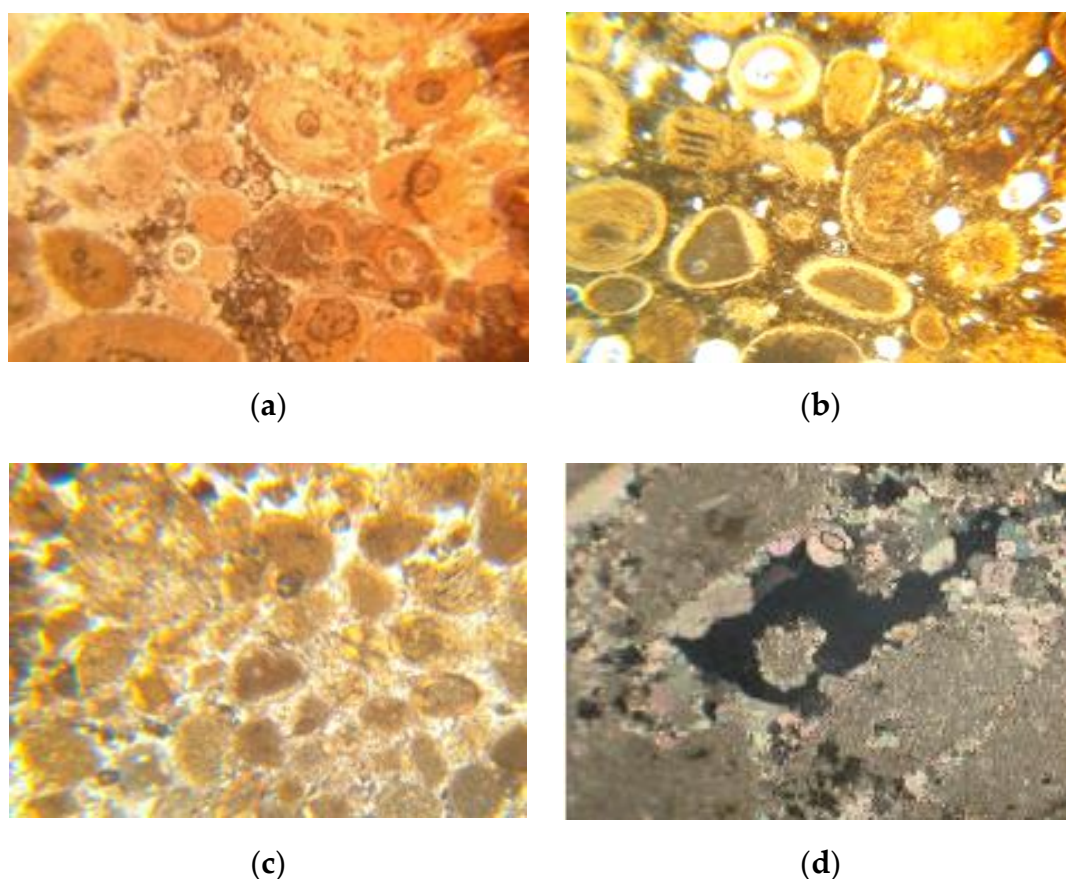


Figure 4. Photomicrographs showing (a,b) lime-Mudstone C.N.; (c) sparry calcite Wackestone C.N.; (d) grainstone and dolomite crystals in fine-grained ground mass C.N.  (for all thin sections, C.N Crossed Nichols).

Additionally, lime-mudstone is the most abundant microfacies type in the Middle Eocene Limestone. It shows a high percentage of mud up to 85% and a rare presence of shells and some skeletal debris [32]. The second microfacies is wackestone, while grains are the main component up to 79%. Wackestone reflects that the sediments in this depositional environment were pointed to moderately agitated water conditions and fair circulation. Consequently, mudstone-wackestone is mainly composed of fine to medium grains embedded in fine materials matrix. Mudstone is recrystallized into sparry calcite and wackestone with dark patches of iron oxides. Furthermore, the depositional environments were distinguished by the studying of the performed thin sections. Three textural classes were detected; firstly, mudstone was deposited near the shore under quiet water, shallow depths, and poor circulation as a result of the fine-grained nature of their sediments [12,14]. The Middle Eocene limestone is characterized by a micritic groundmass, fossils, and microfractures, which are filled with calcite crystals. This Middle Eocene unit was apparently deposited in a transgressive, open sublittoral, warm, and quiet sea [21].

4.3. Physical Rock Properties

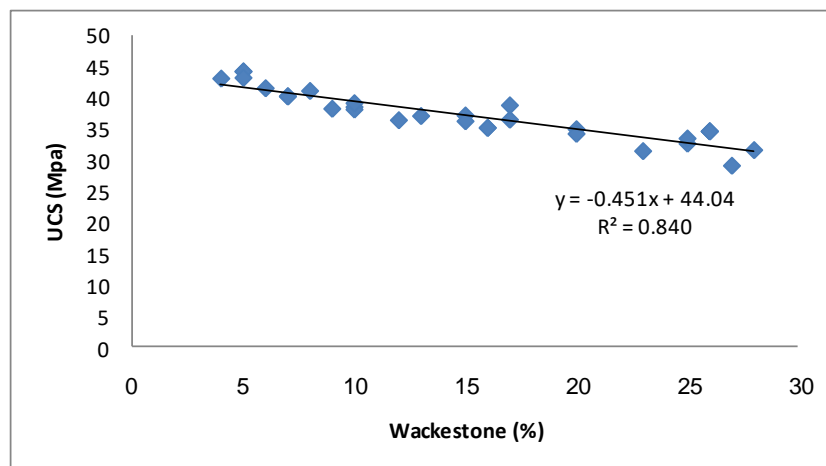
The index properties of the limestone samples along the study site were distinguished. The natural water content ranged from 7.61% to 8.93%. Further, the bulk and dry density were in the range of (2.17–2.19%) and (2.05–2.08%). The specific gravity of the limestone samples ranged from 2.53% to 2.97% (Table 2). Consequently, the absorption rate for the limestone samples ranged from 3.07% to 8.71%. The samples that have low water absorption rates and low saturation degrees are, in general, relatively more durable [33].

Table 2. Index properties of the Middle Eocene limestone samples.

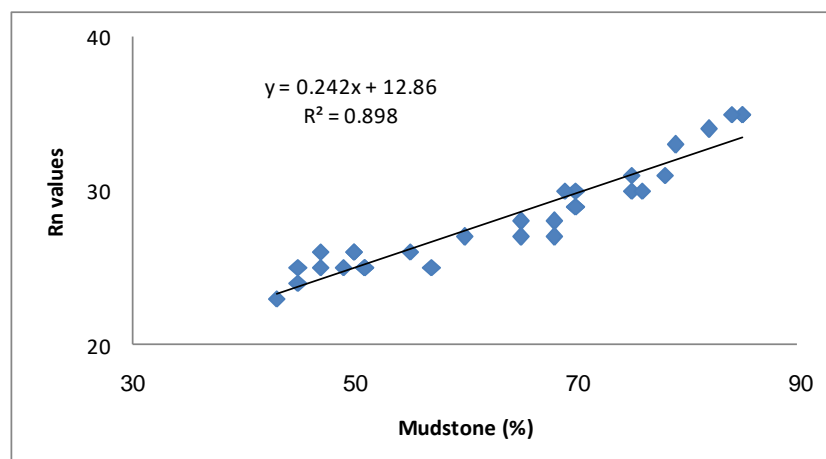
Index Properties	Unit	Result
Specific gravity (Gs)	-	2.53–2.97
Water content (Wc)	%	7.61–8.93
bulk density (γ_{wet})	g/cm^3	2.17–2.19
Dry density (γ_{wet})	g/cm^3	2.05–2.08
Absorption	%	3.07–8.71

4.4. Schmidt Rebound Hammer

Schmidt Rebound hammer Rn-values varied in the range of 23–33 with a mean of 28 and a standard deviation of 3.66 (Table 1). Rn-values have a high positive correlation with mudstone ($R^2 = 0.898$) and a poor positive correlation with dolomite ($R^2 = 0.020$) (Figure 5a,b), while Figure 4c,d indicates moderate inverse relationships with grainstone ($R^2 = 0.747$) and a high negative correlation with wackestone ($R^2 = 0.822$). The strength values from the Schmidt hammer ranges between 30 and 60 MPa and were classified as low to medium strength according to [34].

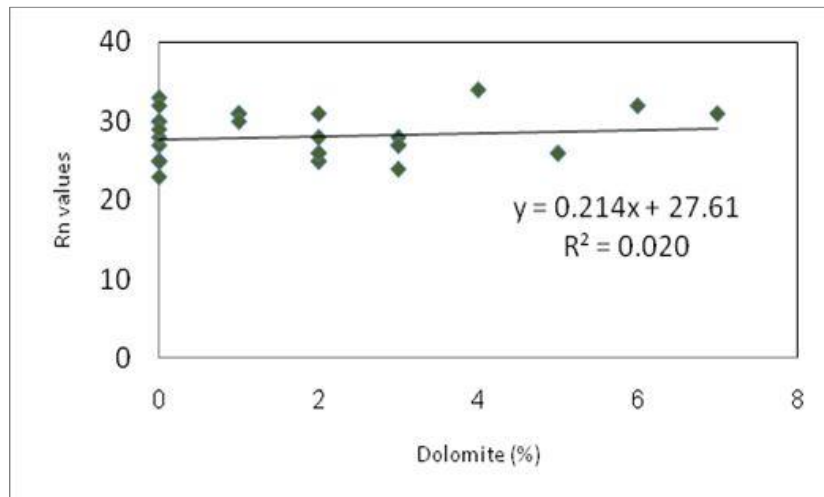


(a)

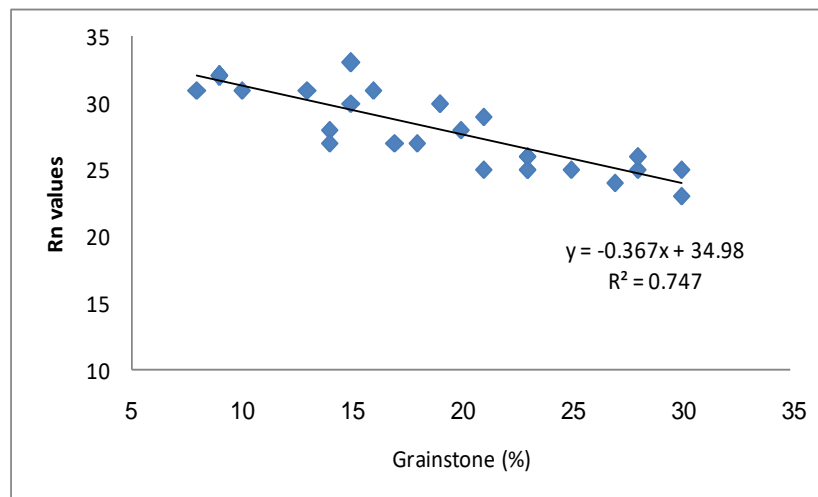


(b)

Figure 5. Cont.



(c)



(d)

Figure 5. Mean Schmidt Rebound hammer values (Rn) with percent of (a) mudstone, (b) dolomite, (c) wackestone, and (d) grainstone.

4.5. Uniaxial Compressive Strength

The UCS for the Middle Eocene Limestone ranges between 29.16 and 43.22 MPa with a mean of 36.29 MPa with a standard deviation of 3.18 (Table 2). The collected samples of the Middle Eocene foundation bedrock were classified according to the engineering classification of [34] as low to medium strength.

The initial part of the curve tends to be slightly concave upward reflecting the closing of microfractures and vugs within the cores (Figure 6). The measured strains during this stage for Middle Eocene limestones represent 40% of total strains. The curves become steeper at higher strains, and the sample exceeds the linear elastic limit giving a nonlinear relationship with gradually reduced values of deformation up to failure. At the end of the curve, large lateral deformations were also clear, compared to those experienced in the initial part. The UCS shows a high and poor direct relationship with mudstone and dolomite ($R^2 = 0.918$ and 0.036), respectively (Figure 7a,b). However, UCS indicates a high negative correlation with wackestone and grainstone ($R^2 = 0.840$ and 0.722) (Figure 7c,d). The UCS was plotted with Rn values (Figure 8). UCS can be determined from Rn; consequently, a positive correlation was estimated between UCS and Rn values. The plots of UCS with Rn indicate a high linear

relationship ($R^2 = 0.885$); on the whole, results were measured realistically to inspect their confidence on the mineralogical constituents of limestone.

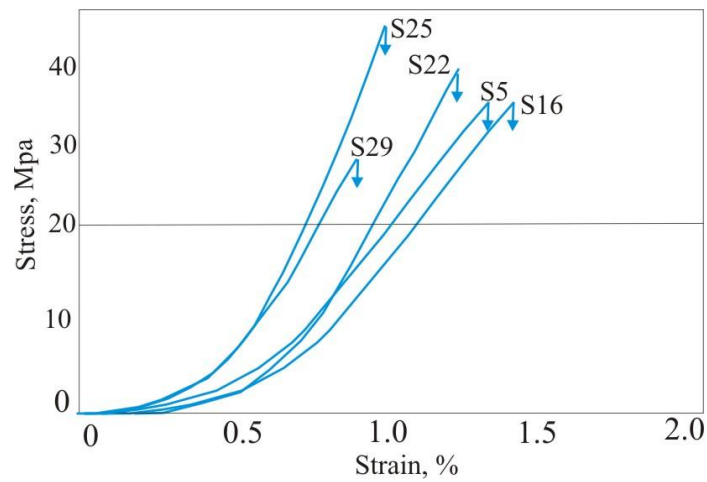
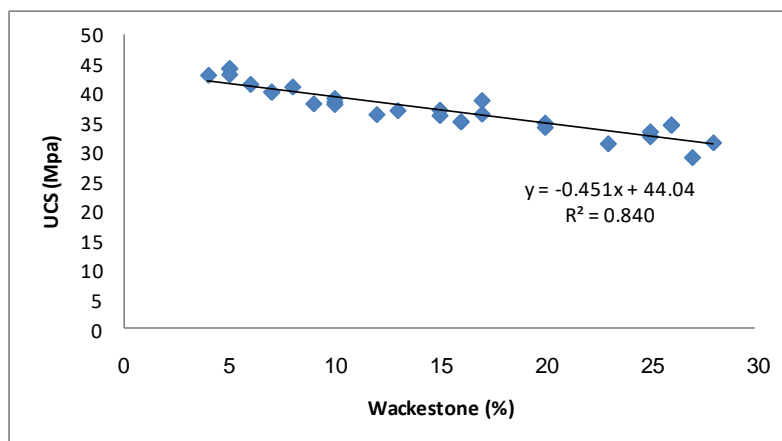
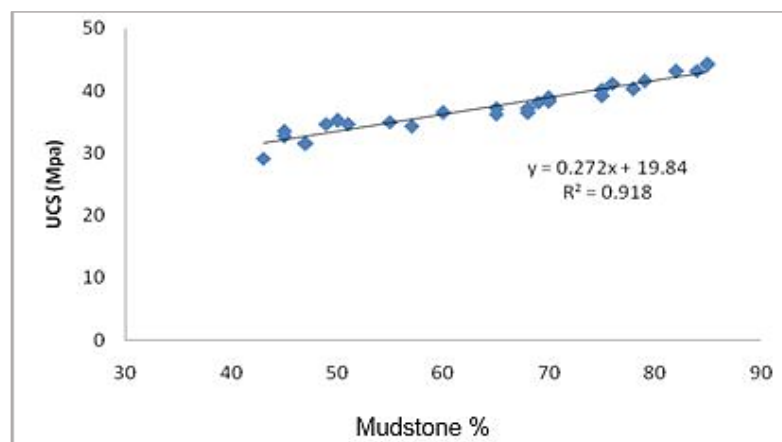


Figure 6. Representative results of uniaxial compressive tests.

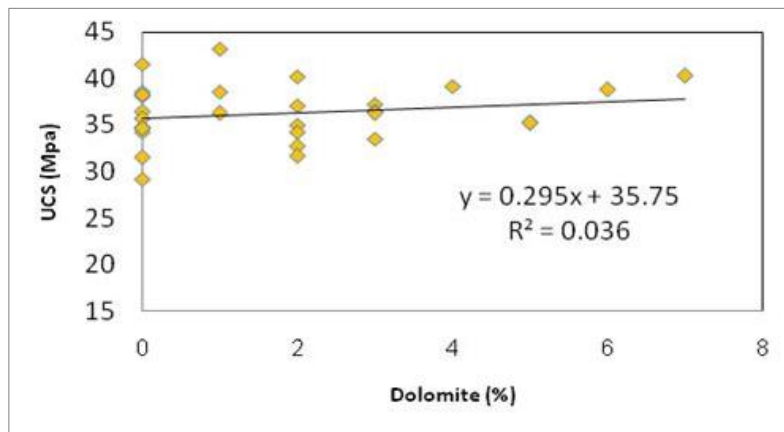


(a)

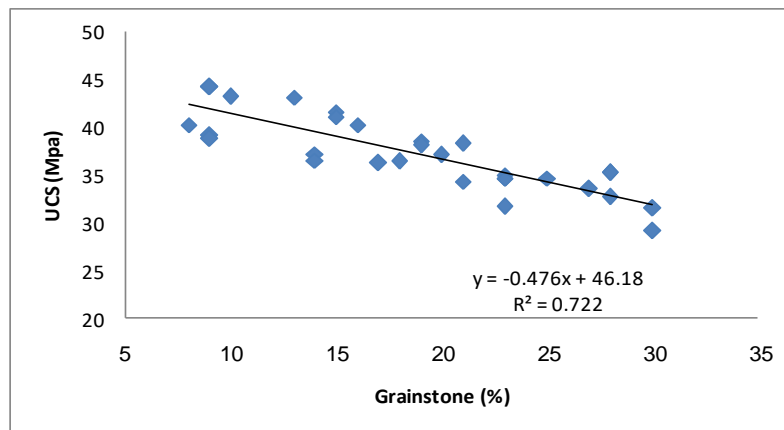


(b)

Figure 7. Cont.



(c)



(d)

Figure 7. Mean UCS with percent of (a) mudstone, (b) dolomite, (c) wackestone, and (d) grainstone.

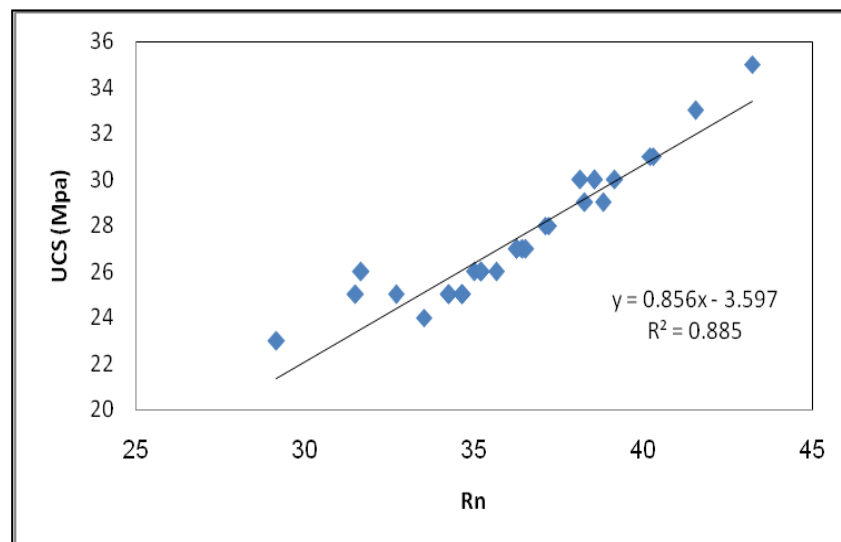


Figure 8. Relationship between a UCS and Rn values.

5. Discussion

The physical properties of the selected samples from the Middle Eocene Limestone foundation bedrock were determined (Table 2). These include bulk density; specific gravity, water content, and absorption rate. The results of these properties point to the fact that water will be unable to make its way into limestone, therefore unable to promote damage in construction model structure [30], which proved that the building material's surface with a low degree of water absorption and porosity will be little or not affected by weathering agents such as wind or rainfall. Supplementarily, the mechanical properties of the Middle Eocene Limestone foundation bedrock were determined by measuring the uniaxial compressive strength and Rn values. UCS and Rn in a straight line interrelated to mudstone, dolomite contents, and vary inversely with wackestone and grainstone (Figure 4). Additionally, mechanical properties are exposing a plain correlation with limestone constituents, but there are interactions with complementary characteristics. Mudstone has an individual express influence and effect on the mechanical behavior of the limestone (Table 1). The highest UCS of 43.22 MPa related to a maximum mudstone content of 85%. Petrographically, the foundation bedrock was texturally classified according to [29] into lime mudstone, wackestone, and mudstone-wackestone. Consequently, the mudstone is the result of cementation of carbonate muds, which consisted of varying percent of aragonite and calcite. Disbanding of aragonite in the argillaceous limestone provided the carbonate for the lithification and cementation of the limestones. The marls, which already underwent a volume decrease by aragonite decrease, lacked cement and became more compacted [22], which indicated high suitability for any construction. However, grainstone and wackestone have had an unhelpful effect on the mechanical properties of the Middle Eocene Limestone.

Accordingly, the lowest UCS (29.16%) value is linked to the highest percentage of grainstone (30%). Furthermore, the break-in grain size between mudstone and microspar is related to the mineralogical composition of the original Limestone-marl alternations, which are widespread forms of carbonate rocks [35,36]. Limestones in these alternations show asymmetrical structure with the highest carbonate content, a very low degree of compaction, and decrease the mechanical properties of the limestone, which leads to unsuitability for constructions. On the other hand, dolomite content individually does not expose the individual behavior with mechanical properties of the Middle Eocene Limestone owing to the lower percentage of it. Further, the contrasting characteristics such as Mudstone + Dolomite result in a high positive effect on the mechanical properties of the Middle Eocene Limestone. All previous interactions between limestone mineral constituents and mechanical parameters exposed moderate to high correlation. These interactions represent an attempt to construct a relationship and a consequential correlation between these parameters for similar rock types in different locations.

6. Conclusions

This study was carried out to investigate the effect of petrographic characteristics on mechanical properties.

Three layers were observed. They were composed of a surface layer that characterizes overburden materials that vary between 0.7 and 3 m. The middle layer is characterized by an argillaceous limestone with thickness ranges between 0.5 to 30 m. The bottom layer is composed of highly argillaceous limestone.

The physical properties proved that the building material's surface has a low degree of water absorption and saturation and is, in general, relatively more durable; the water will be unable to make its way into limestone, therefore unable to promote damage in construction and will be little to not affected by weathering agents such as wind or rainfall.

Petrographically, the investigated Middle Eocene limestone rock samples are texturally classified into lime-mudstone, wackestone, and mudstone-wackestone in different proportions with a high percent of Mudstone.

Analysis of the mechanical properties of the Middle Eocene foundation bedrock indicates low to medium compressive strength (29.16 to 43.22 MPa). It is mainly composed of white, hard limestone

together with a few thin beds of soft marl. The limestone beds are characterized by a low rate of absorption (3.07–8.71), and low water content indicates more durable, evading further compaction, making it suitable for construction.

The UCS shows a high and poor direct relationship with lime-mudstone and dolomite ($R^2 = 0.918$ and 0.036), respectively. Furthermore, it indicates a high negative correlation with wackestone and grainstone ($R^2 = 0.840$ and 0.722)

Rn-values have a high positive correlation with mudstone ($R^2 = 0.898$) and a very poor positive correlation with dolomite ($R^2 = 0.020$). Furthermore, it indicates inverse relationships with grainstone ($R^2 = 0.747$) and wackestone ($R^2 = 0.822$).

The Schmidt Rebound Hammer values demonstrated a high direct relationship with lime-mudstone and a poor direct relationship with dolomite and a high negative correlation with Wackestone and Grainstone.

As a final point, the mineral constituents are considered a major aspect of using them as construction materials as well as the mechanical behavior of limestone. Consequently, petrographic and mechanical properties are dependable for suitability assessment in manufacturing activities.

Author Contributions: Conceptualization, A.E.S. and P.M.; methodology, A.E.S.; software, A.E.S.; validation, A.E.S, P.M., and M.Z.; formal analysis, M.Z.; investigation, A.E.S.; resources, P.M.; data curation, A.E.S.; writing—original draft preparation, A.E.S.; writing—review and editing, M.Z.; visualization, A.E.S.; supervision, P.M.; project administration, M.Z.; funding acquisition, P.M. All authors have read and agreed to the published version of the manuscript.

Funding: This research received no external funding.

Acknowledgments: I am grateful to thank Zagazig Environmental Geophysics Lab (ZEGL) for helping us to perform the laboratory testing. A, El Shinawi would like to express appreciation to Samir Abdeltawab for discussions and valuable great support. Also I would like to thank an anonymous reviewer for suggestions and helpful comments. Thank for the support of project KEGA 059TUKE-4/2019 M-learning tool for intelligent modeling of building site parameters in a mixed reality environment. This work was supported by the Slovak Research and Development Agency under the contract no. APVV-17-0549.

Conflicts of Interest: The authors declare no conflict of interest.

References

- Hala, A.; Mohamed, N.; Mohamed, N. Mapping landslide susceptibility using satellite data and spatial multicriteria evaluation: The case of Helwan District, Cairo. *Appl. Geomat.* **2014**, *6*, 215–228. [[CrossRef](#)]
- Freitas, T.S.; Guimarães, A.S.; Roels, S.; de Freitas, V.P.; Cataldo, A. Is the Time-Domain Reflectometry (TDR) Technique Suitable for Moisture Content Measurement in Low-Porosity Building Materials? *Sustainability* **2020**, *12*, 7855. [[CrossRef](#)]
- El-Shinawi, A. Instability improvement of the subgrade soils by lime addition at Borg El-Arab, Alexandria, Egypt. *J. Afr. Earth Sci.* **2017**, *130*, 195–201. [[CrossRef](#)]
- Miglio, B.; Willmott, T. Durability of stone for construction. In *Journal of ASTM International Selected Technical Papers STP 1514; Durability of Building and construction, Sealants and Adhesives*; ASTM: West Conshohocken, PA, USA, 2010; Volume 3, pp. 241–246.
- Abdeltawab, S. Karst Limestone Geohazards in Egypt and Saudi Arabia. *Int. J. Geoeng.* **2013**, *2*, 258–269. [[CrossRef](#)]
- Akram, M.S.; Farooq, S.; Naeem, M.; Ghazi, S. Prediction of mechanical behavior from mineralogical composition of Sakesar limestone, Central Salt Range, Pakistan. *Bull. Eng. Geol. Environ.* **2017**, *76*, 601–615. [[CrossRef](#)]
- Zeleňáková, M.; Harabinová, S.; Mésároš, P.; Abd-Elhamid, H.; Purcz, P. Modelling of Erosion and Transport Processes. *Water* **2019**, *11*, 2604. [[CrossRef](#)]
- Wilson, J.L. *Carbonate Facies in Geologic History*; Springer: Berlin, Germany, 1975; p. 290.
- Al-Nuaimi, S.; Banawi, A.A.; Al-Ghamdi, S.G. Environmental and Economic Life Cycle Analysis of Primary Construction Materials Sourcing under Geopolitical Uncertainties: A Case Study of Qatar. *Sustainability* **2019**, *11*, 6000. [[CrossRef](#)]

10. Abdelhamid, M.M.A.; Li, D.; Ren, G. Predicting Unconfined Compressive Strength Decrease of Carbonate Building Materials against Frost Attack Using Nondestructive Physical Tests. *Sustainability* **2020**, *12*, 1379. [[CrossRef](#)]
11. Eldeeb, H.; Zelenakova, M. Assessment of the economic value of irrigation water considering achieve main crops self-sufficiency: Case study Sharkia Governorate, Egypt. *Sel. Sci. Pap. J. Civ. Eng.* **2019**, *14*, 39–50. [[CrossRef](#)]
12. Khaled, M.; Abdel Rahman, K.; Khattab, M. Facing the Drilling and Blasting Difficulties at Helwan Quarry, Egypt. *Int. Soc. Explos. Eng.* **2008**, *1*, 1–13.
13. Mohamed, A.M.E.; Sultan, S.A.; Mahmoud, N.I. Delineation of near-surface structure in the southern part of 15th of May City, Cairo, Egypt Using geological, geophysical and geotechnical. *Pure Appl. Geophys.* **2012**, *169*, 1641–1654. [[CrossRef](#)]
14. Majid, T.; Mohammad, R.; Mohammad, B. Engineering properties and durability of limestones used in Persepolis complex, Iran, against acid solutions. *Bull. Eng. Geol. Environ.* **2016**, *75*, 967–978. [[CrossRef](#)]
15. Mohamed, A.M.; Mohamed, A.E.E.A. Mohamed Quarry blasts assessment and their environmental impacts on the nearby oil pipelines, southeast of Helwan City, Egypt. *Nriag J. Astron. Geophys.* **2013**, *2*, 102–115. [[CrossRef](#)]
16. Basheer, A.A.; Atya, M.A.; Shokri, M.; Abu Shady, M.M. Application of ERT and SSR to detect the subsurface cave at 15th May City, Helwan, Egypt. *Nriag J. Astron. Geophys.* **2012**, *1*, 23–32. [[CrossRef](#)]
17. El-Shinawi, A. A comparison of liquid limit values for fine soils: A case study at the north Cairo-Suez district. Egypt. *Geol. Soc. India* **2016**, *89*, 339–343. [[CrossRef](#)]
18. Ghrici, M.; Kenai, S.; Said-Mansour, C. Mechanical properties and durability of mortar and concrete containing natural pozzolana and limestone blended cements. *Cem. Concr. Compos.* **2007**, *29*, 542–549. [[CrossRef](#)]
19. Omar, H.M.; Ismail, N.R. The Suitability of Limestone from Pilaspi Formation (Middle-Late Eocene) for Building Stone in Koya Area, NE Iraq. *ARO* **2015**, *3*, 18–23. [[CrossRef](#)]
20. Kamani, M.; Ajalloeian, R. Evaluation of the mechanical degradation of carbonate aggregate by rock strength tests. *J. Rock Mech. Geotech. Eng.* **2019**, *11*, 121–134. [[CrossRef](#)]
21. Wei, L.; Xianjin, A.; Heping, L. Limestone mechanical deformation behavior and failure mechanisms: A review. *Acta Geochim.* **2018**, *37*, 153–170. [[CrossRef](#)]
22. Munnecke, A.; Kiel, C.S. The Formation of Micritic Limestones and the Development of Limestone-Marl Alternations in the Silurian of Gotland, Sweden. *Facies* **1996**, *34*, 159–176. [[CrossRef](#)]
23. Nabih, M.; El Shinawi, A. Qualitative analysis of clay minerals and swelling potential using gamma-ray spectrometry logs: A case study of the Bahariya Formation in the Western Desert, Egypt. *Appl. Radiat. Isot.* **2020**, *166*, 109384. [[CrossRef](#)] [[PubMed](#)]
24. El-Nahas, F.; Moustafa, A.; Abdel-Tawab, S. Geotechnical characteristics of limestone formations of Gebel Mokattam area. In Proceedings of the First Alexandria Conference on Structural and Geotechnical Engineering, Alexandria, Egypt, 1–3 December 1990; Volume 1, pp. 9–19.
25. ASTM D2216. *Standard Test Methods for Laboratory Determination of Water (Moisture) Content of Soil and Rock by Mass*; ASTM International: West Conshohocken, PA, USA, 2010. [[CrossRef](#)]
26. ASTM D6683. *Standard Test Methods for Measuring Density*; ASTM International: West Conshohocken, PA, USA, 2014. [[CrossRef](#)]
27. ASTM D854. *Standard Test Methods for Specific Gravity of Soil Solids by Water Pycnometer*; ASTM International: West Conshohocken, PA, USA, 2014. [[CrossRef](#)]
28. ASTM D5873. *Standard Testing Method for Determination of Rock Hardness by Rebound Hammer Method*; Annual Book of ASTM Standards; ASTM: West Conshohocken, PA, USA, 2001; Volume 4, p. 9.
29. Dunham, R.J.; Ham, W.E. Classification of carbonate rocks according to depositional texture. Classification of carbonate rocks. *Am. Assoc. Petrol. Geol. Mem.* **1962**, *1*, 108–121.
30. ISRM. *Rock Characterization Testing and Monitoring*; Brown, E., Ed.; Pergamon Press: Oxford, UK, 1981; p. 211.
31. Hoek, E.; Brown, E.T. Empirical strength criterion for rock masses. *J. Geotech. Geoenviron. Eng.* **1980**, *ASCE106 GT9*, 1013–1035.
32. Al-Wosabi, M.; Al-Aydrus, A. Microfacies Analysis and Depositional Environments of Tertiary Carbonate Sequences in Socotra Island, Yemen. *Geol. Bull. Turk.* **2011**, *54*, 57–80.

33. Meng, J.; Pan, J. Correlation between petrographic characteristics and failure duration in clastic rocks. *Eng. Geol.* **2007**, *89*, 258–265. [[CrossRef](#)]
34. Deere, D.U.; Miller, R.P. *Engineering Classification and Index Properties for Intact Rock*; Tech Report AFWL-TR; Air Force Weapons Lab: Bernalillo County, NM, USA, 1966; pp. 65–116.
35. ASTM D2938. *Standard Test Method for Unconfined Compressive Strength of Intact Rock Core Specimens*; ASTM International: West Conshohocken, PA, USA, 1995. Available online: www.astm.org (accessed on 25 May 2020).
36. Einsele, G.; Rickan, W.; Seilacher, A. (Eds.) Cycles and events in stratigraphy—Basic concepts and terms. In *Cycles and Events in Stratigraphy*; Springer: Berlin/Heidelberg, Germany, 1991; pp. 1–19.

Publisher’s Note: MDPI stays neutral with regard to jurisdictional claims in published maps and institutional affiliations.



© 2020 by the authors. Licensee MDPI, Basel, Switzerland. This article is an open access article distributed under the terms and conditions of the Creative Commons Attribution (CC BY) license (<http://creativecommons.org/licenses/by/4.0/>).